



N-heterocyclic carbene Pd(II) complex supported on Fe₃O₄@SiO₂: Highly active, reusable and magnetically separable catalyst for Suzuki-Miyaura cross-coupling reactions in aqueous media

Mitat Akkoç^{a,*}, Nesrin Buğday^b, Serdar Altın^c, Nadir Kiraz^d, Sedat Yaşar^{b,*}, İsmail Özdemir^c

^a Malatya Turgut Özal University, Hekimhan Vocational College, Department of Property Protection and Security, Hekimhan, Malatya, Turkey

^b İnönü University, Faculty of Science and Arts, Department of Chemistry, 44280 Malatya, Turkey

^c İnönü University, Faculty of Science and Arts, Department of Physics, 44280 Malatya, Turkey

^d Akdeniz University, Faculty of Science and Arts, Department of Chemistry, Antalya, Turkey

ARTICLE INFO

Article history:

Received 3 February 2021

Revised 11 March 2021

Accepted 7 April 2021

Available online 16 April 2021

Keywords:

Magnetic palladium catalyst
Pd(II)-N-heterocyclic carbene complex
Suzuki-Miyaura reaction
Green chemistry
Magnetite

ABSTRACT

A new type magnetic nano Fe₃O₄@SiO₂@NHC@Pd-MNPs heterogeneous catalyst was fabricated and characterized by Fourier Transform Infrared (FTIR) spectroscopy, Transmission Electron Microscopy (TEM), X-Ray Diffraction (XRD), X-ray Photoelectron Spectroscopy (XPS), Energy Disperse X-ray analysis (EDX), Thermogravimetric Analysis (TGA), Differential Thermal Analysis (DTA), and Scanning Electron Microscopy (SEM). The loading amount of Palladium (Pd) to magnetic nano Fe₃O₄@SiO₂@NHC@Pd-MNPs was measured by Inductively Coupled Plasma-Optical Emission Spectroscopy (ICP-OES) analysis. The catalytic activity of magnetic nano Fe₃O₄@SiO₂@NHC@Pd-MNPs heterogeneous catalyst was examined on Suzuki-Miyaura cross-coupling reactions of aryl halides with different substituted arylboronic acid derivatives. All coupling reactions yielded excellent results and high TOF (up to 76528 h⁻¹) in the presence of 2 mg of Fe₃O₄@SiO₂@NHC@Pd-MNPs catalyst (0.0197 mmolg⁻¹, 0.00394 mmol%Pd) at 80 °C in 2-propanol/H₂O (1:2). In addition, the magnetic nano Fe₃O₄@SiO₂@NHC@Pd-MNPs catalyst was easily recovered by using an external Nd-magnet and reused for the Suzuki cross-coupling reactions. The catalyst showed strong structural and chemical stability and was reused six times without losing its catalytic activity substantially.

© 2021 Elsevier B.V. All rights reserved.

1. Introduction

Magnetic nanoparticles (MNPs) have gained a lot of attention in recent years due to their superior properties and wide range of applications in the areas such as electronics, sensors, memory devices and medical applications [1]. Compare to other fields, the applications of MNPs in the medical field are quite high because of their superparamagnetic properties, low toxicity, biocompatibility and have high magnetic susceptibility [2–12]. In recent years, there have been significant challenges in the development of materials with such superior properties. However, due to their chemical activity, robustness and reusability, the MNPs are used as either support materials or active components in catalysis.

Carbon nanomaterials, polymer materials, metal oxides, Metal-Organic Frameworks (MOFs), Zeolitic Imidazolate Frameworks

(ZIFs) and silica derivatives are mostly used as support materials for transition-metal catalysts and organo-catalysts. Among them, silica-supported transition-metal catalysts have been preferred more than other support materials in terms of preparation, utilization and applications. However, silica is used as a protective layer. Metal oxides can be protected by silica to prepare M_xO_y@SiO₂ structures. For this reason, Fe₃O₄ core and silica shell have recently gained great interest. Fe₃O₄@SiO₂ has unique chemical and physical properties such as chemically functional surface and magnetic response. Thus, Fe₃O₄@SiO₂ is a strong support material for the preparation of heterogeneous catalysts [13–19]. The superiority of the Fe₃O₄@SiO₂ material supported catalysts is that the catalyst can be easily separated from the reaction medium by applying an external magnet [20].

Due to their superior characteristics, the N-heterocyclic carbenes (NHC) have recently gained substantial interest as an alternative to phosphine ligand [21]. NHCs are one of the most known versatile ligands for transition metals because of their strong σ-donor property and the ease of structural modification in the design of homogeneous and heterogeneous catalysts. The

* Corresponding authors.

E-mail addresses: mitat.akkoc@ozal.edu.tr (M. Akkoç), sedat.yasar@inonu.edu.tr (S. Yaşar).

σ -donor capacities of NHCs ligands differ depend on the type of NHC. Szostak et al. found the sigma donor properties of different types of NHC ligands different. In this study, diaminocarbene and cyclic (alkyl) (amino) carbene show the strongest sigma donor capacity [22]. Furthermore, 6-membered NHCs (IPr and IMes) are significantly stronger sigma-donors than their 5-membered parent IPr and IMes analogues. In the same study, it was stated that the N-alkyl-benzimidazol-2-ylidene NHC precursor has better sigma donor property than N-alkyl-imidazol-2-ylidenes [22]. In this study, the $^1J_{CH}$ coupling constant of 1-(2,3,4,5,6-pentamethylbenzyl)-3-(ethanol)-benzimidazolium iodine, which we used as the NHC ligand precursor, is found as 219,16 Hz. This value found is in agreement with the relevant literature and shows that similar σ -donor capacities than N-alkyl-imidazol-2-ylidenes analogues.

NHCs bind to metal centers stronger than phosphines, complexes formed are more stable toward air, moisture and heat in many applications [23–25]. This may help the stability of Metal-NHC complexes under catalytic and biological conditions. The combination of NHCs and MNPs is very important for the synthesis of new types of MNPs catalysts. To date, several complexes immobilized on the MNPs have been successfully synthesized and used as catalysts for C-C bond formation reactions [26–40]. Dong et al. synthesized a supported Pd(II) complex on magnetite core-shell of $Fe_3O_4@SiO_2$ for Suzuki-Miyaura cross-coupling reaction [40]. They claimed that their catalyst's reusability is high and can catalyze the Suzuki reaction six times without a significant decrease of the catalyst performance at 80 °C in EtOH. Khazaei et al. prepared nano- $Fe_3O_4@SiO_2$ supported Pd(0) nanocatalyst and used as a catalyst on Suzuki coupling reaction of aryl iodide and aryl bromide with aryl boronic acid derivatives in the presence of CaO as a base at 85 °C in aqueous media [41]. This catalyst can also show high catalytic activity and reusability without loss on catalytic activity after five runs. Fafee et al. also prepared $Fe_3O_4@SiO_2$ supported Vitamin B1-Pd complex and investigated its catalytic activity on Suzuki coupling of aryl halides at 60 °C in EtOH [28]. They reported good to high yields of coupled products of aryl halides with substituted phenylboronic acid derivatives. Also, catalyst reported showed five reusabilities with slight loss of its activity. Tao et al. synthesized magnetic nanoparticle-supported N-heterocyclic carbene-palladacycle (SMNP@NHC-Pd) and investigated its catalytic activity on Suzuki-Miyaura cross-coupling reaction of heterocyclic 9-chloroacridine with diverse boronic acids. They reported that

0.5–1 mol% catalyst efficiently catalyze the reactions and resulted in high yields at 100 °C in 24 h.

Herein, we reported synthesis and characterization of $Fe_3O_4@SiO_2$ -based MNPs catalysts and investigated the catalytic activity of it on Suzuki-Miyaura cross-coupling reaction under mild reaction conditions in aqueous media.

0.5–1 mol% catalyst efficiently catalyze the reactions and resulted in high yields at 100 °C in 24 h.

Herein, we reported synthesis and characterization of $Fe_3O_4@SiO_2$ -based MNPs catalysts and investigated the catalytic activity of it on Suzuki-Miyaura cross-coupling reaction under mild reaction conditions in aqueous media.

2. Experimental section

2.1. General considerations

Otherwise stated, all synthesis was carried out in aerobic conditions. All chemicals and solvents purchased from sigma Aldrich, Fluorochem and BLDpharm chemical companies and used as obtained. For NMR analysis, a Bruker Avance III 400 MHz NMR spectrometer was used at room temperature with the decoupled nucleus, using $CDCl_3$ and $DMSO-d_6$ as a solvent and referenced versus TMS as standard. Coupling constants (J values) are given in

hertz. NMR multiplicities are abbreviated as follows: s = singlet, d = doublet, t = triplet, m = multiplet signal. All reactions were monitored on a Shimadzu GC2010 Plus system by GC-FID with an HP-5 column of 30 m length, 0.32 mm diameter, and 0.25 mm film thickness. Some of the catalytic products were previously reported. New compounds were characterized by different spectroscopic techniques. See Supporting Information section. The GC-MS analysis of compounds was performed on a Shimadzu GC-MS 2010 plus using a TRX-5 column on positive ESI mode. The FTIR analysis was performed with a PerkinElmer Spectrum 100 GladiATR FT/IR spectrometer. The crystal structure analysis of the synthesized powder was performed by an X-ray diffractometer labeled Rigaku Rint 2000 which powered by $Cu K_{\alpha}$ radiation was used for characterization. The scan rate was chosen as 2°/min between 2° and 80°/min. The microstructural properties and the surface morphology of the synthesized powders were investigated by Leo EVO-40 VPX scanning electron microscope (SEM). For XPS analyse: XPS instrument: PHI 5000 VersaProbe II, X rays: $hn = 1486,6$ eV monochromatic, spot 200 μm and Energy resolution (hi-resolution spectra): 0.8 eV were used. The TEM analyses were performed by FEI TECNAI OSIRIS operating at 200 kV, Morphological analysis with HAADF-STEM imaging mode, Chemical analysis with the Super-X EDX detector system (4 SDD detectors).

2.2. General procedure for Suzuki-Miyaura cross-coupling reaction

Aryl halide (0.5 mmol), aryl boronic acid (0.6 mmol), potassium carbonate (1 mmol), and palladium nano-catalyst (2 mg, 0.00394 mmol% Pd) was placed in a flask under air and 3 ml of 2-propanol/water mixture (1:2, v:v) was added to flask and stirred in a preheated oil bath (80 °C) for an appropriate time. After completion reaction, the reaction was cooled to room temperature and the palladium nano-catalyst was removed by an external magnet from the reaction mixture. Then, the reaction was diluted with 3 ml of water and 3 ml of ethyl acetate. The organic phase was separated by extraction and dried over $MgSO_4$, and filtrated and the filtrate evaporated under reduced pressure to obtain crude product. The pure products were purified by column chromatography using ethyl acetate/hexane as the eluent (1:30).

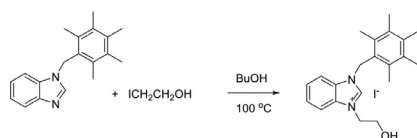
2.3. Synthesis

2.3.1. Synthesis of NHC salt

(1-(2,3,4,5,6-pentamethylbenzyl)-3-(ethanol)-benzimidazolium iodine)

The NHC salt was synthesized by the following reported procedure [42a,b]. 2-iodoethanol (1.8 g; 110 mmol) was added to 10 mL *n*-BuOH solution of 1-(2,3,4,5,6-pentamethylbenzyl)benzimidazole (2.78 g; 100 mmol). Then, the reaction solution was refluxed for 4 h. After the reaction cooled to room temperature, yellow crystals were obtained. Crystals were removed from the solution by filtration, washed with diethyl ether (5 × 5 mL) and dried under vacuum. Yellow crystals were characterized by 1H and ^{13}C NMR spectroscopy.

Yield: 75%, 1H NMR (400 MHz, $DMSO-d_6$) $\delta = 8.97$ (s, 1H, NCHN), 8.19 and 8.12 (d, $J = 28$ Hz, 4H, C_6H_4), 5.72 (s, 2H, $CH_2C_6(CH_3)_5-2,3,4,5,6$), 5.02 (s, 1H, CH_2CH_2OH), 4.54 (t, $j = 4.6$ Hz, 2H, CH_2CH_2OH), 3.74 (m, 2H, CH_2CH_2OH), 2.27 (s, 3H, $CH_2C_6(CH_3)_5-2,3,4,5,6$), 2.24 (s, 6H, $CH_2C_6(CH_3)_5-2,3,4,5,6$), 2.21 (s, 6H, $CH_2C_6(CH_3)_5-2,3,4,5,6$). ^{13}C NMR (100 MHz, $DMSO-d_6$) $\delta = 141.8, 137.8, 134.4, 133.4, 132.1, 131.9, 127.1, 127.0, 125.9, 114.6, 114.3, 59.1, 49.8, 46.8, 17.5, 17.2, 16.9$. Elemental analysis for $C_{21}H_{27}N_2OI$: %Calc. C: 56.01, H: 6.04, N: 6.22; %found C: 56.12, H: 6.14, N: 6.38.



Scheme 1. Synthesis pathway of the $\text{Fe}_3\text{O}_4@SiO_2@NHC@Pd^0$ -MNPs catalyst, **3**.

2.4. Synthesis of silica-coated magnetic nanoparticle NHC-Pd catalyst, $\text{Fe}_3\text{O}_4@SiO_2@NHC@Pd^0$ -MNPs

Fe_3O_4 was synthesized via the reported co-precipitation method with little modifications using $\text{FeCl}_3 \cdot 6\text{H}_2\text{O}$ and $\text{FeCl}_2 \cdot 4\text{H}_2\text{O}$ [43]. The synthesized Fe_3O_4 nanoparticles were coated with silica by tetraethylorthosilicate (TEOS) to fabricate $\text{Fe}_3\text{O}_4@SiO_2$ nanoparticles. This nanoparticle functionalized with 1-ethanol-3-(2,3,4,5,6-pentamethylbenzyl)benzimidazolium hydroiodide in methanol under reflux conditions to obtain $\text{Fe}_3\text{O}_4@SiO_2@NHC$. Finally, the interaction of $\text{Pd}(\text{OAc})_2$ with $\text{Fe}_3\text{O}_4@SiO_2@NHC$ in 50 mL acetonitrile under reflux conditions for 24 hours resulted in the formation of $\text{Fe}_3\text{O}_4@SiO_2@NHC@Pd^0$ -MNPs catalyst labeled as **3** (Scheme 1). As a result of the ICP-OES analysis, it was determined that our $\text{Fe}_3\text{O}_4@SiO_2@NHC@Pd^0$ -MNPs catalyst contains 0.21 wt% Pd (0.0197 mmol/g).

3. Result and discussions

3.1. FTIR analysis

The $\text{Fe}_3\text{O}_4@SiO_2@NHC@Pd$ and other chemical components used in the catalyst were first analyzed by FTIR spectroscopy. The FTIR spectrum of NHC, Fe_3O_4 , $\text{Fe}_3\text{O}_4@SiO_2$ and $\text{Fe}_3\text{O}_4@SiO_2@NHC@Pd$ as shown in Fig 1. The band at 584 cm^{-1} is belonged to Fe–O bonds and the peak at 3421 cm^{-1} associated with the O–H groups [40,41]. The absorption bands at 1091, 799 and 464 cm^{-1} were attributed to Si–O–Si antisymmetric stretching vibrations, Si–O–Si symmetric stretching and Si–O–Si or O–Si–O, respectively. According to FT-IR analysis, it shows that we have coated Fe_3O_4 with a silica layer with success. The FT-IR spectra of NHC give bands at 3506 (OH stretching), 2970 (CH (C_6H_2) stretching), 2937 [CH(CH_2 - CH_2) stretching] and 1600, 1400, 1300 cm^{-1} . The characteristic spectral for NHC is the intense peak at 3506 cm^{-1} , due to the supposition of the OH bending vibration. After connection of NHC to $\text{Fe}_3\text{O}_4@SiO_2$ and $\text{Fe}_3\text{O}_4@SiO_2@NHC@Pd$ the bands at 3506 cm^{-1} were disappeared and these results indicate that functionalization of $\text{Fe}_3\text{O}_4@SiO_2$ with NHC successfully done. The shift of absorption band at 1560 cm^{-1} (CNC stretching

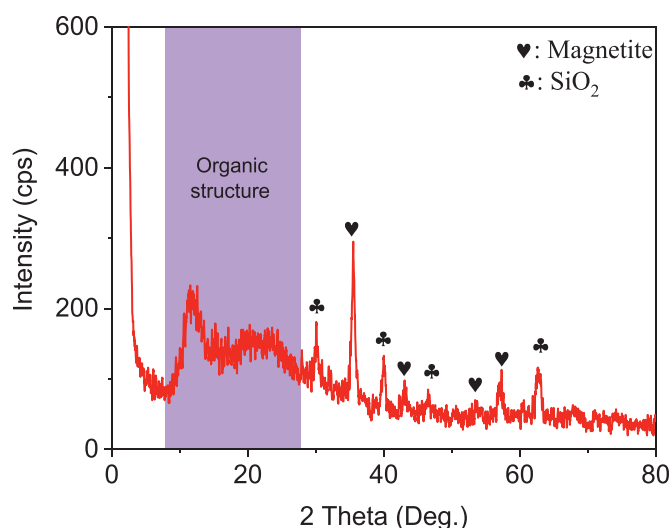


Fig. 2. XRD pattern of $\text{Fe}_3\text{O}_4(\text{Magnetite})@SiO_2@NHC@Pd$ -MNPs.

of benzimidazole) to 1394 cm^{-1} is suggesting the formation of Pd–C bond (Pd–CNC stretching of benzimidazole) after reaction with $\text{Pd}(\text{OAc})_2$.

3.2. XRD analysis

The second characterization of the catalyst was done by XRD analysis. The powder XRD pattern of the of $\text{Fe}_3\text{O}_4@SiO_2@NHC@Pd$ -MNPs presented in Fig. 2 gives information related to three phases as magnetite (Fe_3O_4), SiO_2 , and organic structure. In this prepared $\text{Fe}_3\text{O}_4@SiO_2@NHC@Pd$ -MNPs, the Fe_3O_4 as a central component and SiO_2 layer for protect magnetite and NHC–Pd attached to SiO_2 over this structure. The XRD peaks at 30.08, 40.02, 48.64 and 62.83 are due to (110), (011), (120), and (220) reflection planes of the SiO_2 phase (JCPDF number: 45-1374). Similarly, the peaks of 35.42, 43.05, 53.40, and 56.9 are related to (311), (400), (422) and (511) reflection planes of magnetite (JCPDF number: 19-0629). The wide halo around 8–28° may be due to the amorphous form of SiO_2 on magnetite and organic ligands in the structure. It also may be due to the nano-structured formation of $\text{Fe}_3\text{O}_4@SiO_2@NHC@Pd$ -MNPs as seen in reported literature [26].

3.3. SEM and TEM and EDX analysis

The characterization of the catalyst was also done by SEM and TEM techniques. The morphology and size of the

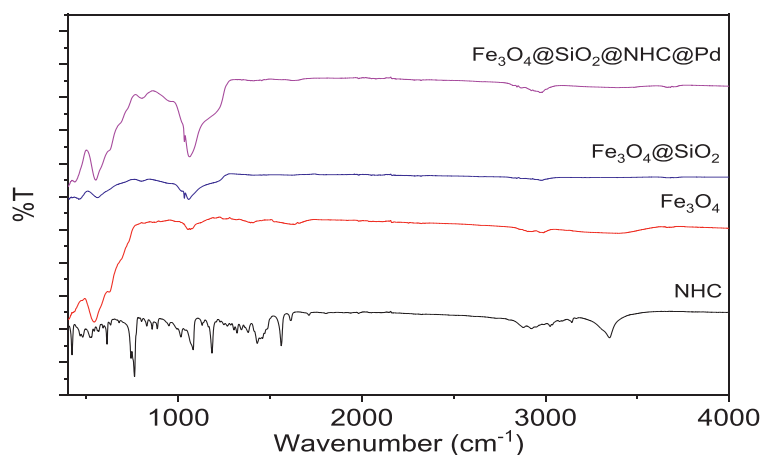


Fig. 1. FT-IR spectra of $\text{Fe}_3\text{O}_4@SiO_2@NHC@Pd$ -MNPs catalyst and its constituent components.

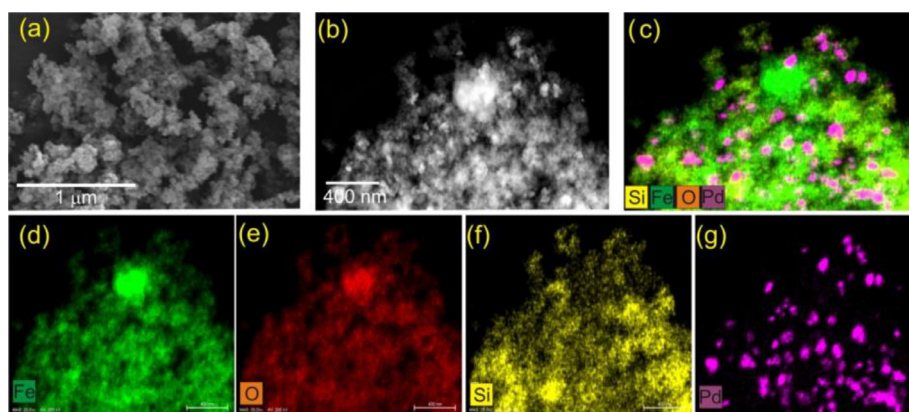


Fig. 3. (a) SEM, (b) TEM images of $\text{Fe}_3\text{O}_4@SiO_2@NHC@Pd$, (c) EDX-dot mapping and (d), (e), (f) and (g) elemental distribution of Fe, O, Si and Pd, respectively.

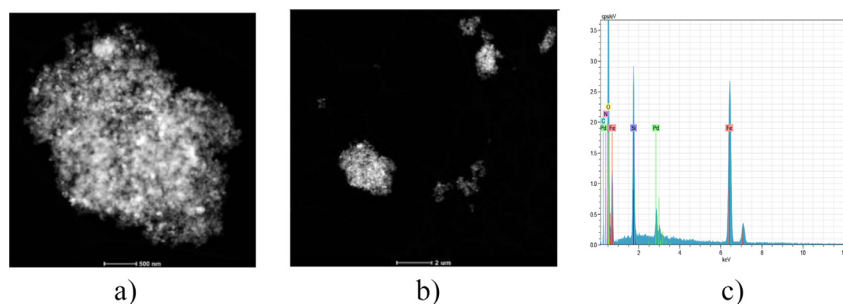


Fig. 4. a) and b) The TEM image of $\text{Fe}_3\text{O}_4@SiO_2@NHC@Pd$ -MNPs c) SEM-EDX spectrum of $\text{Fe}_3\text{O}_4@SiO_2@NHC@Pd$ -MNPs.

$\text{Fe}_3\text{O}_4@SiO_2@NHC@Pd$ -MNPs were obtained by SEM and TEM analysis. Fig. 3a shows the SEM images of the powders at 60kX magnification. It is seen that there are spherical type grain formation and the size of the particles are in nm range size with a cluster-type formation in the solid form. To see the particle size in more detail, the HAADF-STEM images of the $\text{Fe}_3\text{O}_4@SiO_2@NHC@Pd$ -MNPs powders were investigated as seen in Fig. 3b. The particle size was measured as below 10 nm and some of them are around 40–60 nm (Fig. 3). According to the TEM images (Fig. 4a), the Pd metal species are seem well dispersed and composed in nano-sized particles between 20–35 nm range.

The elemental distribution of ions in the powder and chemical analysis based on the elements are presented in Fig. 3c–g. It is observed that the distribution of Si, Fe, and O shows homogeneous behavior which is the expected result for the study and it was proven by EDX. It should be noted that the observation of well-dispersed Pd particles is seen in the figures which is an expected behavior for catalytic studies.

The elemental composition of the $\text{Fe}_3\text{O}_4@SiO_2@NHC@Pd$ -MNPs was also analyzed by Energy Dispersive X-ray spectroscopy (EDX) spectrum. The EDX results reveal the presence of the elemental composition of NHC (C, Si, O, N) and Pd elements in the $\text{Fe}_3\text{O}_4@SiO_2@NHC@Pd$ -MNPs catalyst surface (Fig. 4b). Also, elemental mapping of $\text{Fe}_3\text{O}_4@SiO_2@NHC@Pd$ shows the dispersion of Pd on the texture. As a result of the ICP-OES analysis, the exact amount of Pd in our $\text{Fe}_3\text{O}_4@SiO_2@NHC@Pd$ -MNPs was found 0.21 wt% Pd ($0.0197 \text{ mmol g}^{-1}$).

3.4. XPS analysis

The structural characterization of the catalyst was further clarified by using the X-ray photoelectron spectroscopy (XPS) analysis method. The XPS spectra of $\text{Fe}_3\text{O}_4@SiO_2@NHC@Pd$ -MNPs and each ion spectra present in Figs. 5 and 6, respectively. The

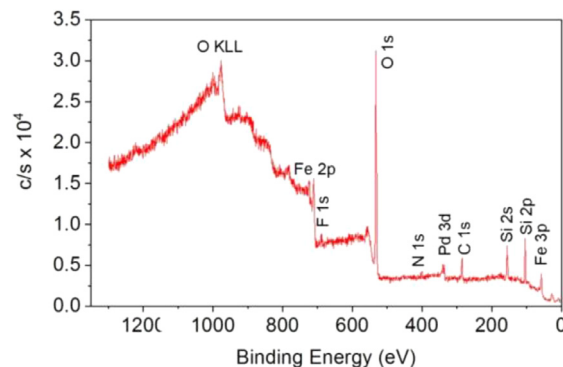
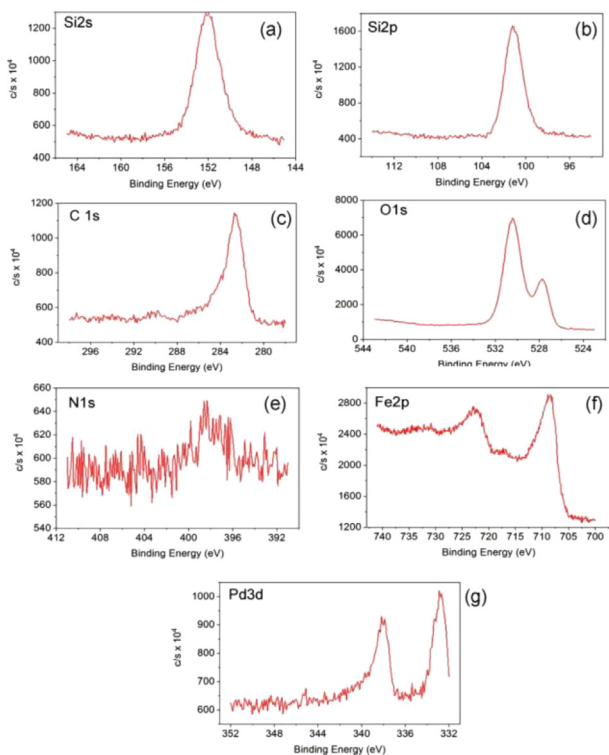


Fig. 5. XPS spectra of $\text{Fe}_3\text{O}_4@SiO_2@NHC@Pd$ -MNPs.

XPS spectrum was investigated by the aspect of all layers in the $\text{Fe}_3\text{O}_4@SiO_2@NHC@Pd$. The XPS peaks of SiO_2 were given in Figs. 5 and 6a–b. The Si2s, Si2p, C1s and O1s electrons were observed at 152, 102, 285 and 527 eV, respectively (Fig. 6a–d). The energy level of C1s in Fig. 6c is related to C–C/C=C bonds in the structure [44]. The N1s electron peak at 398 eV in Fig. 6e is due to imidazolate-N atom in the structure [45]. These data show the presence of the atoms mentioned in the structure of the synthesized catalyst [46]. The another peak at 531 eV for O1s belongs to the O atom in the NHC ligand which has a -1 oxidation state [47]. It shows that Fe3p demonstrate the presence of Fe ions and Fe2p split into two energy level at ~708 eV for 2p_{1/2} and ~721 eV for 2p_{3/2} (Fig. 6e) and it can be explained by the formation of Fe²⁺ and Fe³⁺ in the structure which is an expected result for magnetite [48]. Fig. 6g exhibits the XPS spectra of the Pd element and gives two peaks at 333.2 and 338.4 eV which correspond to 3d_{5/2} and 3d_{3/2} orbitals of metallic state Pd⁰ rather than Pd(II) [49].

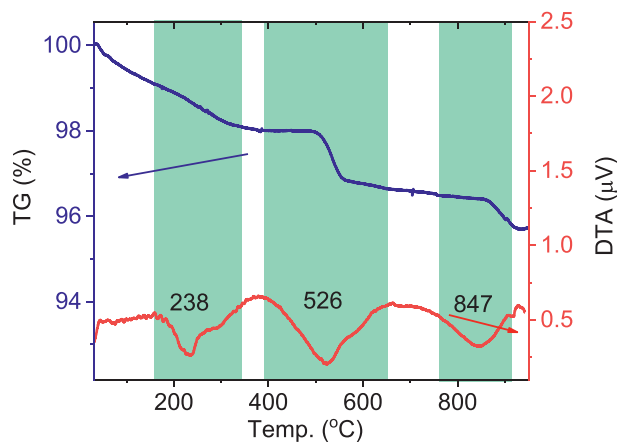
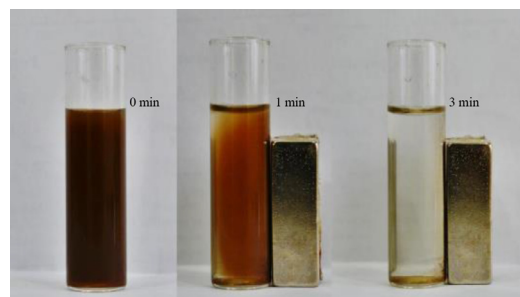
Table 1Atomic concentration values of $\text{Fe}_3\text{O}_4@\text{SiO}_2@\text{NHC}@\text{Pd-MNPs}$ catalyst determined by XPS analysis.

Sample	N 1s (%.at)	C 1s (%.at)	O 1s (%.at)	Si 2p (%.at)	Fe 2p (%.at)	Pd 3d _{3/2} (%.at)
$\text{Fe}_3\text{O}_4@\text{SiO}_2@\text{NHC}@\text{Pd-MNPs}$	0.57	12.57	62.89	15.22	8.23	0.52

**Fig. 6.** XPS spectra of (a) Si2s, (b) Si2p, (c) C1s, (d) O1s, (e) N1s, (f) Fe2p and (g) Pd3d.

Unlike the literature [28], these results show that Pd^{2+} is reduced to metallic palladium during the synthesis process due to the heat applied. This reduction process may be promoted by the weak σ -donor ability of NHC ligand. Szostak et al., have calculated the sigma donor capability of the different NHC ligands and they indicated that the sigma donor capability can be estimating from the coupling constants of $^1J_{\text{CH}}$ in ^{13}C NMR [22]. CH J-coupling value can in principle be calculated both the ^1H -coupled ^{13}C NMR spectrum and from the ^{13}C satellites of the ^1H NMR spectrum [50,51] Based on this information, the $^1J_{\text{CH}}$ coupling constant of the NHC precursor we used in this study is calculated 219.16 Hz from the ^{13}C satellites of the ^1H NMR spectrum. This value is the average value when compared to the values obtained from other NHC precursors [22]. This sigma donor property of NHC may have played a role in reducing Pd^{2+} to Pd^0 . The reduction of Pd (II) to metallic palladium from the reaction medium without any specific reduction process and the presence of only one type of Pd in the medium is a desired situation for synthesis of Pd nanomaterials without using extra reducing agents.

The atomic concentration of $\text{Fe}_3\text{O}_4@\text{SiO}_2@\text{NHC}@\text{Pd-MNPs}$ catalyst was determined by XPS analysis presented in Table 1. According to XPS result, $\text{Fe}_3\text{O}_4@\text{SiO}_2@\text{NHC}@\text{Pd-MNPs}$ catalyst contains 0.52 wt%, 0.0488 mmol/g Pd^0 . The difference between the ICP-OES and XPS results may be due to the XPS analysis determining the amount of Pd^0 metal present on the surface. However, ICP-OES analysis determines the amount of Pd in the catalyst with higher accuracy. Thus, we used ICP-OES to analyze results in the calculation of Pd loadings.

**Fig. 7.** DTA and TGA curve of $\text{Fe}_3\text{O}_4@\text{SiO}_2@\text{NHC}@\text{Pd-MNPs}$ catalyst.**Fig. 8.** Magnetization of the $\text{Fe}_3\text{O}_4@\text{SiO}_2@\text{NHC}@\text{Pd-MNPs}$ catalyst in the *i*-PrOH when an external magnetic field is applied.

3.5. DTA and TGA analysis

The thermal stability of $\text{Fe}_3\text{O}_4@\text{SiO}_2@\text{NHC}@\text{Pd-MNPs}$ catalyst was evaluated by thermal gravimetric analysis-differential thermal analysis (DTA and TGA) and presented in Fig. 7.

DTA and TG analysis shows that there are three regions for both data which are related to endothermic activity in the samples. The first reaction at 238 °C should be due to the decomposition of the $\text{Fe}_3\text{O}_4@\text{SiO}_2@\text{NHC}@\text{Pd-MNPs}$ which corresponds to the highest temperature for the stability of samples. The other two reactions are the transition should be the formation of a new phase with losing some oxygen and nitrogen ions from the structure. So, it should be noted that the $\text{Fe}_3\text{O}_4@\text{SiO}_2@\text{NHC}@\text{Pd-MNPs}$ can stable without any decomposition and it can be used in catalytic reactions of temperature up to 238 °C.

The catalyst has a very high magnetization due to the magnetite in the structure of the catalyst support material. Fig. 8 shows that when an external magnetic field is applied, the catalyst shows high magnetization in a short time.

3.6. Catalytic studies

We examined the catalytic activity of $\text{Fe}_3\text{O}_4@\text{SiO}_2@\text{NHC}@\text{Pd-MNPs}$ catalyst, **3**, for the Suzuki-Miyaura cross-coupling reaction. First, we conducted a series of experiments to find out the optimum conditions for the catalytic system. A series experiments

Table 2
Optimization of the conditions of phenylboronic acid and 4-bromoacetophenone catalyzed by $\text{Fe}_3\text{O}_4@\text{SiO}_2@\text{NHC@Pd-MNPs}$, **3**.

Entry	[Cat]	Base	Solvent	Temp./Time	Yield %
1	[3], 1 mg	K_2CO_3	$\text{H}_2\text{O}/i\text{-PrOH}$	80 °C, 5 min.	92
2	[3], 1 mg	K_2CO_3	$\text{H}_2\text{O}/i\text{-PrOH}$	50 °C, 5 min.	22
3	[3], 1 mg	K_2CO_3	$\text{H}_2\text{O}/i\text{-PrOH}$	25 °C, 5 min.	8
4	[3], 2 mg	K_2CO_3	$\text{H}_2\text{O}/i\text{-PrOH}$	80 °C, 5 min.	99
5	[3], 2 mg	NaOH	$\text{H}_2\text{O}/i\text{-PrOH}$	80 °C, 5 min.	42
6	[3], 2 mg	Na_2CO_3	$\text{H}_2\text{O}/i\text{-PrOH}$	80 °C, 5 min.	60
7	[3], 2 mg	Cs_2CO_3	$\text{H}_2\text{O}/i\text{-PrOH}$	80 °C, 5 min.	45
8	[3], 2 mg	K^tOBu	$\text{H}_2\text{O}/i\text{-PrOH}$	80 °C, 5 min.	38
9	[3], 2 mg	KOH	$\text{H}_2\text{O}/i\text{-PrOH}$	80 °C, 5 min.	25
10	[3], 2 mg	K_2CO_3	H_2O	80 °C, 5 min.	22
11	[3], 2 mg	K_2CO_3	<i>i</i> -PrOH	80 °C, 5 min.	5
12	[3], 2 mg	K_2CO_3	EtOH	80 °C, 5 min.	3
13	[3], 2 mg	K_2CO_3	DMF	80 °C, 5 min.	20
14	[3], 2 mg	K_2CO_3	Dioxane	80 °C, 5 min.	12
15	[3], 2 mg	K_2CO_3	DMF/ H_2O	80 °C, 5 min.	55
16	[3], 2 mg	K_2CO_3	$\text{H}_2\text{O}/\text{EtOH}$	80 °C, 5 min.	88
17	[3], 2 mg	K_2CO_3	$\text{H}_2\text{O}/\text{Dioxane}$	80 °C, 5 min.	65
18	[3], 2 mg	K_2CO_3	$\text{H}_2\text{O}/i\text{-PrOH}$	80 °C, 5 min.	- ^b
19	[3], 2 mg	K_2CO_3	$\text{H}_2\text{O}/i\text{-PrOH}$	80 °C, 6 h.	20 ^b
20	$\text{Pd}(\text{OAc})_2$, 0,0088 mg	K_2CO_3	$\text{H}_2\text{O}/i\text{-PrOH}$	80 °C, 5 min.	53
21	PdCl_2 , 0,007 mg	K_2CO_3	$\text{H}_2\text{O}/i\text{-PrOH}$	80 °C, 5 min.	45
22	$\text{Pd}(\text{OAc})_2$, 0,0088 mg	K_2CO_3	$\text{H}_2\text{O}/i\text{-PrOH}$	80 °C, 5 min.	- ^b
23	PdCl_2 , 0,007 mg	K_2CO_3	$\text{H}_2\text{O}/i\text{-PrOH}$	80 °C, 5 min.	- ^b
24	-	K_2CO_3	$\text{H}_2\text{O}/i\text{-PrOH}$	80 °C, 5 min.	trace

^aReaction conditions: **3** (2 mg, 0.00394 mmol%Pd), phenylboronic acid (0.6 mmol), 4-bromoacetophenone (0.5 mmol), Base (1.0 mmol), solvent 3 ml. ^b 4-Chloroacetophenone was used. GC yields determine according to 4-bromoacetophenone or 4-chloroacetophenone using (trifluoromethyl)benzene as an internal standard.

were performed to find out the effective amount of catalyst, the suitable solvent or solvent mixtures and base. In these reactions, the 4-bromoacetophenone and phenylboronic acid were selected as a substrates. To find the effective amount of catalyst and reaction time we tried catalytic reaction catalyzed by different catalyst loading at 25 °C, 50 °C and 80 °C (Table 2, entry 1-3). According to the results, 2 mg catalyst loading give highest yield at 80 °C in short time. After determining the specific catalyst loading and reaction temperature, the next step is find out the appropriate base (Table 2, entry 4-9). Different polar solvents were also tested solely or as a solvent mixture (Table 2, entry 10-17). According to our previously reported results [52–60], DMF, 2-propanol, EtOH, Dioxane, DMF-water (1:1), 2-propanol-water (1:2) were selected as a solvent. The carbonate-derived bases such as Na_2CO_3 , K_2CO_3 , Cs_2CO_3 were tried first due to their good solubility in aqueous media. The best catalytic activity was obtained with 2-propanol-water (1:2) and K_2CO_3 solvent-base couple. Other solvents and bases also give moderate to good yield. Then, 4-chloroacetophenone was used as a substrate to understand the effectiveness of the catalyst or to show the applicability of the catalytic system to chlorinated aryl halides (Table 1, entries 18-19). No product formation was observed in the reaction performed under the same reaction conditions with the 4-chloroacetophenone substrate (Table 1, entry 18). In the reaction for 6 h, a very low yield of product formation was observed (Table 1, entry 19). For comparison, different commercially available palladium sources such as PdCl_2 and $\text{Pd}(\text{OAc})_2$ were tested at the same concentration in the catalytic system we created. From the results we obtained, it was seen that the catalyst we synthesized had much better activity than commercially available palladium sources (Table 1, entries 20-23). As a result of the reaction without catalyst, trace amount of product formation was observed (Table 1, entry 24).

As a result of all these different reactions conditions, the optimum conditions for the catalytic system described here as follows: 0.5 mmol Ar-Br, 0.6 mmol boronic acid, 2 mg of **3**

(0.0394 mmol%Pd), 1 mmol K_2CO_3 , 2-propanol-water (1:2, w/w) at 80 °C.

The optimized reaction condition on hand, Suzuki-Miyaura cross-coupling of different aryl bromides with different phenylboronic acid derivatives were examined (Table 3) First, different *p*-substituted aryl bromides contain CN, NO_2 , COCH_3 , CH_3 , OCH_3 , CF_3 with phenylboronic acid, 4-tert-buthylboronic acid, 2-methoxyboronic acid and 3-formyl-4-methoxyboronic acid were investigated. The results clearly showed that the reaction can be completed in 5-30 min with moderate to excellent yields for both electron-donating and electron-withdrawing substituted aryl bromides and phenylboronic acids. It has been observed that the Suzuki coupling of aryl bromides with electron-donating groups and phenylboronic acids take a longer time when compared to aryl bromides containing electron-withdrawing groups. It may be due to the electronic effect of electron-donating substituents. However, *o*-substituted aryl bromides and boronic acid derivatives need more reaction time due to steric hindrance of the substituted group. Moreover, heteroaryl bromides were also tried with these phenylboronic acid derivatives and the result were satisfied with high mono or diarylated selectivity (Table 3). The products contain heteroaryl groups may be important for biologically active applications.

3.7. Reusability studies

The reusability of the catalyst was investigated with a set of experiments via a used catalyst with 4-bromoacetophenone under optimized reaction condition for the Suzuki coupling reaction. After the first run, the catalyst was recovered from reaction media with the external magnet and washed with a sufficient amount of ethanol and water. After final washing with ethanol, the catalyst was dried at 80 °C for 12 h and used for the next reaction. For each new reaction, new substrates were used. These processes were tried 6 times consecutively and the results are presented in Fig. 9. According to the results, there was no significant decrease

Table 3
Suzuki-Miyaura cross-coupling of aryl bromides with substituted phenylboronic acids derivatives catalyzed by **3**.

Entry	Ar-B(OH) ₂	Ar-Br	Product	Time (min)	^a Yield %	TON/TOF (h ⁻¹)
1				10	99	6345/37691
2				10	99	6382/37912
3				30	55 ^b	6379/7017
4				30	89	6379/11355
5				5	99	6377/75762
6				5	99	6282/74637
7				5	93	6430/71759
8				15	95	6275/23847
9				5	90	6275/67777
10				5	96	6392/73640
11				10	99	6381/37907
12				15	100	6425/25703
13				30	38	6345/4822
14				30	66	6382/8424
15				30	59	6379/7527
16				30	99 ^c	6377/12627
17				5	94	6282/70867
18				5	91	6430/70215
19				30	65	6276/8158
20				5	84	6276/63259
21				5	88	6392/67504
22					5	92
23				30	100	6382/12765
24				30	100	6379/12759
25				5	100 ^c	6377/76528
26				5	99	6282/74637
27				5	99	6430/76389
28				30	45	6276/5648
29				30	80	6275/10041
30				5	73	6392/55998
31				10	70	6382/26803
32					15	81
				13		

(continued on next page)

Table 3 (continued)

33				10	92	6345/35027
34				10	84	6382/32168
35				10	87	6379/33300
36				5	65 ^c	6377/49743
37				20	78	6276/14685
38				30	85	6377/10841
39				30	83	6276/10418
40				30	90	6283/11309
41				30	85	6430/10931
42				15	75	6426/19277

^a Reaction conditions: **3** (0.00394 mmol% Pd), phenylboronic acid (0.6 mmol), aryl bromide (0.5 mmol), Base (1.0 mmol), *i*-PrOH/water (1:2, 3 mL), 80 °C. GC yields determine according to aryl bromide using (trifluoromethyl)benzene as an internal standard.

^b 50 °C.

^c Room temperature.

Table 4

Comparison results of Fe₃O₄@SiO₂@NHC@Pd-MNPs with reported catalyst on the Suzuki-Miyaura reactions for 4-bromobenzonitrile with phenylboronic acid.

Ref.	Cat. (mol%), Solvent, Temperature	Time(min)	Yield (%)
55	CMC-NHC-Pd (0.8 mol%), EtOH/H ₂ O (1:1), 60 °C, X=Br, X*=Cl	180, 300*	94, 52*
56	γ-Fe ₂ O ₃ -acetamidine-Pd, DMF, 100 °C, X=Br	120, 30*	92, 96*
57	Cell-NHC-Pd (0.75 mol%), DMF/H ₂ O (1:1), 80 °C, X=Br	120	99
58	Pd/C-NHC-P(OR) ₃ (0.03 mol%), EtOH, 80 °C, X=Br	60	98
28	Fe ₃ O ₄ @SiO ₂ @VB1-Pd NPs (0.022 mol%), EtOH, 60 °C, X=Br	20, 20*	98, 95*
26	Fe ₃ O ₄ @SiO ₂ -NHC-Pd ^(III) (0.37 mol%), H ₂ O, 60 °C, X=I	60, 90*	92, 93*
59	Pd-TEG, (0.005 mol%) H ₂ O, 25 °C, X=Br	840	91
60	(Pd ^{II} -NHC) _n @SiO ₂ (0.27 mol%), DMF/H ₂ O (2:1), 60 °C, X=Br	8*	95*
This work	Fe ₃ O ₄ @SiO ₂ @NHC@Pd-MNPs (0.00394 mmol%, <i>i</i> -PrOH/H ₂ O (1:2), 80 °C, X=Br	5, 10*	90, 99*

* Yield obtained for 4-bromobenzene substrate.

* Yield obtained for 4-chlorobenzene substrate.

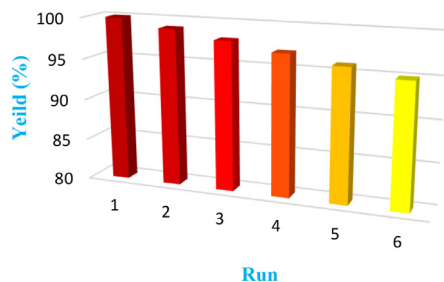


Fig. 9. Recyclability of the catalyst **3** for the Suzuki-Miyaura cross-coupling reaction.

in yield and catalytic performance of the catalyst after 6 trials. Although, it is not entirely possible to transfer the entire catalyst amount to the next reaction with an externally applied magnetic field. This small problem can cause a slight drop in product yields (5% reduction in yield after 6 runs).

3.8. Hot filtration test study

Furthermore, to understand the palladium leaching, a hot filtration test was performed. There was no increase in the amount of the yield after GC analysis while the reaction continued after the catalyst was removed from the reaction medium. The concentrations of recovered catalyst after 6 runs were found by ICP-OES analysis as 0.20 wt%, which indicated that the leaching of Pd from the support material is very limited and thus does not affect catalyst performance significantly. Herein, the M-NHC strong covalent bond strength may play a role in the stability of catalyst. To see the changes in the structure of the used catalyst, SEM and EDX analysis was performed during each time. SEM and EDX results shows that there are very limited structural changes and agglomeration on the catalyst (Figure S3).

After many catalytic reactions, our Fe₃O₄@SiO₂@NHC@Pd-MNPs catalyst has showed high catalytic activity on the Suzuki-Miyaura cross-coupling reaction for a variety of boronic acids and different aryl bromides.

3.9. Comparison with the literature

Comparing the activities of our catalyst and similar types of silica-supported magnetic or non-magnetic heterogeneous palladium catalysts in Suzuki reactions [55–60], it is seen that our catalyst has better catalytic activity and application utility (in terms of separation of the catalyst from the reaction medium, catalyst loading and reusability) than many reported catalyst (Table 4). As far as we know, the amount of the Pd in the catalyst used has not been reported in the literature so far. Considering the amount of catalyst used and the yield obtained, it appears that the catalyst has an extraordinary activity. Although our catalytic system positively differentiated from reported catalytic systems, the disadvantage of the catalytic system in this study is almost ineffective with aryl chloride substrates under same reaction conditions. From these results, we hope that this catalyst can be used as a catalyst for other organic transformation reactions where palladium catalysts use.

4. Conclusions

In summary, an efficient and green $\text{Fe}_3\text{O}_4@SiO_2@NHC@Pd$ -MNPs catalyst was successfully synthesized and applied for the Suzuki-Miyaura cross-coupling reaction to synthesize fine substituted and biological important biaryls. This novel catalyst showed very high catalytic activity in Suzuki-Miyaura cross-coupling reactions with high reusability without loss of activity. This catalyst has high strong magnetic and disperse properties. Due to these properties, it helps increase catalytic activity and recovery of catalyst from reaction media. Stability towards air and moisture, low catalyst loading, easy handling and recyclability of this catalyst are some of its unique characteristics. The applicability of this catalyst in other palladium-catalyzed catalytic systems is under research in our lab and we expect that it will provide high catalytic activity with reusability in other reactions as well.

Compliance with ethical standards

Conflict of interest: The author declared no conflict of interest.

Declaration of Competing Interest

The authors declare that they have no known competing financial interests or personal relationships that could have appeared to influence the work reported in this paper.

Acknowledgments

Authors would like to thanks to NFFA for XPS and TEM studies which performed in France (CEA LETI/DTSI/SCMC Grenoble Cedex 9 FRANCE and thanks to N. GAMBACORTI for organization of XPS and TEM analysis) within the framework of the NFFA-Europe Transnational Access Activity (NFFA Project ID: 723).

Supplementary materials

Supplementary material associated with this article can be found, in the online version, at doi:10.1016/j.jorganchem.2021.121823.

References

- [1] S. Sun, C.B. Murray, D. Weller, L. Folks, A. Moser, Monodisperse FePt nanoparticles and ferromagnetic FePt nanocrystal superlattices, *Science* 287 (2000) 1989–1992, doi:10.1126/science.287.5460.1989.
- [2] Y. Chen, H.R. Chen, L.M. Guo, Q.J. He, F. Chen, J. Zhou, J. Feng, J. Shi, Hollow/rattle-type mesoporous nanostructures by a structural difference-based selective etching strategy, *ACS Nano* 4 (2010) 529–539, doi:10.1021/nn901398j.
- [3] D. Shi, H.S. Cho, Y. Chen, H. Xu, H. Gu, J. Lian, W. Wang, G. Liu, C. Huth, L. Wang, R.C. Ewing, S. Budko, G.M. Pauletti, Z. Dong, Fluorescent polystyrene- Fe_3O_4 composite nanospheres for in vivo imaging and hyperthermia, *Adv. Mater.* 21 (2009) 2170–2173, doi:10.1002/adma.200803159.
- [4] A.A. Jafari, H. Mahmoudi, H. Firouzabadi, A copper acetate/2-aminobenzenthiole complex supported on magnetite/silica nanoparticles as a highly active and recyclable catalyst for 1,2,3-triazole synthesis, *RSC Adv.* 5 (2015) 107474–107481, doi:10.1039/C5RA22909J.
- [5] S.J. Zhang, X.H. Liu, L.P. Zhou, W.J. Peng, Magnetite nanostructures: One-pot synthesis, superparamagnetic property and application in magnetic resonance imaging, *Mater. Lett.* 68 (2012) 243–246, doi:10.1016/j.matlet.2011.10.070.
- [6] H. Firouzabadi, N. Iranpoor, M. Gholinejad, J. Hoseini, Magnetite (Fe_3O_4) nanoparticles-catalyzed Sonogashira-Hagihara reactions in ethylene glycol under ligand-free conditions, *Adv. Synth. Catal.* 353 (2011) 125–132, doi:10.1002/adsc.201000390.
- [7] M. Esmailpour, J. Javidi, Magnetically-recoverable schiff base complex of Pd (II) immobilized on $\text{Fe}_3\text{O}_4@SiO_2$ nanoparticles: An efficient catalyst for Mizoroki-Heck and Suzuki-Miyaura coupling reactions, *J. Chin. Chem. Soc.* 62 (2015) 614–626, doi:10.1002/jccs.201500013.
- [8] H. Zhang, X. Zhong, J.J. Xu, H.Y. Chen, Fe_3O_4 /polypyrrole/Au nanocomposites with core/shell/shell structure: synthesis, characterization, and their electrochemical properties, *Langmuir* 24 (2008) 13748–13752, doi:10.1021/la8028935.
- [9] Q. Dong, G. Li, C.-L. Ho, M. Faisal, C.-W. Leung, P.W.-T. Pong, K. Liu, B.-Z. Tang, I. Manners, W.-Y. Wong, A Polyferroplatinyne precursor for the rapid fabrication of L10-FePt-type Bit patterned media by nanoimprint lithography, *Adv. Mater.* 24 (2012) 1034–1040 doi.org/10.1002/adma.201104171.
- [10] Q. Dong, Z. Meng, C.-L. Ho, H. Guo, W. Yang, I. Manners, L. Xu, W.-Y. Wong, A molecular approach to magnetic metallic nanostructures from metallopolymer precursors, *Chem. Soc. Rev.* 47 (2018) 4934–4953, doi:10.1039/C7CS00599G.
- [11] Z. Meng, G. Li, S.-C. Yiu, N. Zhu, C.-W. Leung, Z.-Q. Yu, I. Manners, W.-Y. Wong, Nanoimprint lithography-directed self-assembly of bimetallic Iron-M (M = Palladium, Platinum) complexes for magnetic patterning, *Angew. Chem. Int. Ed.* 59 (2020) 11521–11526 doi.org/10.1002/anie.202002685.
- [12] Z. Wei, D. Wang, Y. Liu, X. Guo, Y. Zhu, Z. Meng, Z.-Q. Yu, W.-Y. Wong, Ferrocene-based hyperbranched polymers: synthetic strategy for shape control and applications as electroactive materials and precursor-derived magnetic ceramics, *J. Mater. Chem. C* 8 (2020) 10774–10780 doi.org/10.1039/D0TC01380C.
- [13] N. Insin, J.B. Tracy, H. Lee, J.P. Zimmer, R.M. Westervelt, M.G. Bawendi, Incorporation of iron oxide nanoparticles and quantum dots into silica microspheres, *ACS Nano* 2 (2008) 197–202, doi:10.1021/nn700344x.
- [14] M. Esmailpour, J. Javidi, N.F. Dodeji, H. Hassannezhad, $\text{Fe}_3\text{O}_4@SiO_2$ -polymer-imid-Pd magnetic porous nanosphere as magnetically separable catalyst for Mizoroki-Heck and Suzuki-miyaura coupling reactions, *J. Iran Chem. Soc.* 11 (2014) 1703–1715, doi:10.1007/s13738-014-0443-5.
- [15] A. Abou-Hassan, R. Bazzi, V. Cabuil, Multistep continuous-flow microsynthesis of magnetic and fluorescent γ - $\text{Fe}_2\text{O}_3@SiO_2$ core/shell nanoparticles, *Angew. Chem. Int. Ed.* 48 (2009) 7180–7183, doi:10.1002/anie.200902181.
- [16] M. Esmailpour, J. Javidi, $\text{Fe}_3\text{O}_4@SiO_2$ -imid-PMAN magnetic porous nanosphere as reusable catalyst for synthesis of polysubstituted quinolines under solvent-free conditions, *J. Chin. Chem. Soc.* 62 (2015) 328–334, doi:10.1002/jccs.201400380.
- [17] X.Q. Xu, C.H. Deng, M.X. Gao, W.J. Yu, P.Y. Yang, M.X. Zhang, Synthesis of magnetic microspheres with immobilized metal ions for enrichment and direct determination of phosphopeptides by matrix-assisted laser desorption/ionization mass spectrometry, *Adv. Mater.* 18 (2006) 3289–3293, doi:10.1002/adma.200601546.
- [18] Y.H. Deng, D.W. Qi, C.H. Deng, X.M. Zhang, D.Y. Zhao, Superparamagnetic high-magnetization microspheres with an $\text{Fe}_3\text{O}_4@SiO_2$ core and perpendicularly aligned mesoporous SiO_2 shell for removal of microcystins, *J. Am. Chem. Soc.* 130 (2008) 28–29, doi:10.1021/ja0777584.
- [19] M. Esmailpour, J. Javidi, M. Zandi, One-pot synthesis of multisubstituted imidazoles under solvent-free conditions and microwave irradiation using $\text{Fe}_3\text{O}_4@SiO_2$ -imid-PMAN magnetic porous nanospheres as a recyclable catalyst, *New J. Chem.* 39 (2015) 3388–3398, doi:10.1039/C5NJ00050E.
- [20] G. Toskas, C. Cherif, R.D. Hund, E. Laourine, A. Fahmi, B. Mahltig, Inorganic/organic (SiO_2)/PEO hybrid electrospun nanofibers produced from a modified sol and their surface modification possibilities, *ACS Appl. Mater. Interfaces* 3 (2011) 3673–3681, doi:10.1021/am200858s.
- [21] Q. Zhao, G. Meng, S.P. Nolan, M. Szostak, N-heterocyclic carbene complexes in C–H activation reactions, *Chem. Rev.* 120 (2020) 1981–2048 doi.org/10.1021/acs.chemrev.9b00634.
- [22] G. Meng, L. Kakalis, S.P. Nolan, M. Szostak, A simple 1H NMR method for determining the σ -donor properties of N-heterocyclic carbenes, *Tetrahedron Lett.* 60 (2019) 378–381, doi:10.1016/j.tetlet.2018.12.059.
- [23] P.D. Stevens, G. Li, J. Fan, M. Yen, Y. Gao, Recycling of homogeneous Pd catalysts using superparamagnetic nanoparticles as novel soluble supports for Suzuki, Heck, and Sonogashira cross-coupling reactions, *Chem. Commun.* (2005) 4435–4437, doi:10.1039/B505424A.
- [24] K.V.S. Ranganath, J. Kloesges, A. Schfer, F. Glorius, Asymmetric nanocatalysis: N-heterocyclic carbenes as chiral modifiers of $\text{Fe}_3\text{O}_4/Pd$ nanoparticles, *Angew. Chem.* 122 (2010) 7952–7956, doi:10.1002/ange.201002782.
- [25] M.N. Hopkinson, C. Richter, M. Schedler, F. Glorius, An overview of N-heterocyclic carbenes, *Nature* 510 (2014) 485–496, doi:10.1038/nature13384.

- [26] M. Esmaeilpour, A.R. Sardarian, H. Firouzabadi, N-Heterocyclic carbene-Pd(II) complex based on theophylline supported on Fe₃O₄@SiO₂ nanoparticles: Highly active, durable and magnetically separable catalyst for green Suzuki-Miyaura and Sonogashira-Hagihara coupling reactions, *J. Organomet. Chem.* 873 (2018) 22–34, doi:10.1016/j.jorganchem.2018.08.002.
- [27] K.V.S. Ranganath, A.H. Schfer, F. Glorius, Comparison of superparamagnetic Fe₃O₄-supported N-heterocyclic carbene-based catalysts for enantioselective allylation, *Chem. Cat.Chem.* 3 (2011) 1889–1891, doi:10.1002/cctc.201100201.
- [28] F. Rafiee, N. Mehdizadeh, Palladium N-heterocyclic carbene complex of vitamin B1 supported on silica-coated Fe₃O₄ nanoparticles: A green and efficient catalyst for C–C coupling, *Catal. Lett.* 148 (2018) 1345–1354, doi:10.1007/s10562-018-2363-y.
- [29] Y. Zheng, P.D. Stevens, Y. Gao, Magnetic nanoparticles as an orthogonal support of polymer resins: applications to solid-phase Suzuki cross-coupling reactions, *J. Org. Chem.* 71 (2006) 537–542, doi:10.1021/jo051861z.
- [30] D. Wang, W. Liu, F. Bian, W. Yu, Magnetic polymer nanocomposite-supported Pd: an efficient and reusable catalyst for the Heck and Suzuki reactions in water, *New J. Chem.* 39 (2015) 2052–2059, doi:10.1039/C4NJ01581A.
- [31] M. Gholinejad, M. Razeghi, C. Najera, Magnetic nanoparticles supported oxime palladacycle as a highly efficient and separable catalyst for room temperature Suzuki-Miyaura coupling reaction in aqueous media, *RSC Adv.* 5 (2015) 49568–49576, doi:10.1039/C5RA05077D.
- [32] B. Karimi, F. Mansouri, H. Vali, A highly water-dispersible/magnetically separable palladium catalyst based on a Fe₃O₄@SiO₂ anchored TEG-imidazolium ionic liquid for the Suzuki-Miyaura coupling reaction in water, *Green Chem.* 16 (2014) 2587–2596, doi:10.1039/C3GC42311E.
- [33] H. Liu, P. Wang, H. Yang, J. Niu, J. Ma, Palladium supported on hollow magnetic mesoporous spheres: a recoverable catalyst for hydrogenation and Suzuki reaction, *New J. Chem.* 39 (2015) 4343–4350, doi:10.1039/C5NJ00104H.
- [34] A. Ghorbani-Choghamarani, G. Azadi, Fe₃O₄@SiO₂@l-arginine@Pd(0): A new magnetically retrievable heterogeneous nanocatalyst with high efficiency for C–C bond formation, *Appl. Organometal. Chem.* 30 (2016) 247–252, doi:10.1002/aoc.3424.
- [35] F. Zhang, M. Chen, X. Wu, W. Wang, H. Li, Highly active, durable and recyclable ordered mesoporous magnetic organometallic catalysts for promoting organic reactions in water, *J. Mater. Chem. A* 2 (2014) 484–491, doi:10.1039/C3TA13446F.
- [36] T.M. Dhameiliya, H.A. Donga, P.V. Vaghela, B.G. Panchal, D.K. Sureja, K.B. Bodiwala, M.T. Chhabria, A decenary update on applications of metal nanoparticles (MNPs) in the synthesis of nitrogen- and oxygen-containing heterocyclic scaffolds, *RSC Adv.* 10 (2020) 32740–32820, doi:10.1039/D0RA02272A.
- [37] Q. Deng, Y. Shen, H. Zhua, T. Tu, A magnetic nanoparticle-supported N-heterocyclic carbene-palladacycle: an efficient and recyclable solid molecular catalyst for Suzuki-Miyaura cross-coupling of 9-chloroacridine, *Chem. Commun.* 53 (2017) 13063–13066, doi:10.1039/C7CC06958H.
- [38] I. Yavari, A. Mobaraki, Z. Hosseinzadeh, N. Sakhaee, Copper-catalyzed Mizoroki-Heck coupling reaction using an efficient and magnetically reusable Fe₃O₄@SiO₂@PrNCu catalyst, *J. Organomet. Chem.* 897 (2019) 236–246 doi.org/10.1016/j.jorganchem.2019.06.029.
- [39] A. Kilic, E. Gezer, F. Durap, M. Aydemir, A. Baysal, Pd(II) supported dioxime functionalized Fe₃O₄ nanoparticles as efficient, eco-friendly and reusable catalysts for the Suzuki-Miyaura cross-coupling reaction in water, *J. Organomet. Chem.* 896 (2019) 129–138 doi.org/10.1016/j.jorganchem.2019.06.007.
- [40] X. Le, Z. Dong, Z. Jin, Q. Wang, J. Ma, Suzuki-Miyaura cross-coupling reactions catalyzed by efficient and recyclable Fe₃O₄@SiO₂@mSiO₂-Pd(II) catalyst, *Catal. Commun.* 53 (2014) 47, doi:10.1016/j.catcom.2014.04.025.
- [41] A. Khazaei, M. Khazaei, M. Nasrollahzadeh, Nano-Fe₃O₄@SiO₂ supported Pd(0) as a magnetically recoverable nanocatalyst for Suzuki coupling reaction in the presence of waste eggshell as low-cost natural base, *Tetrahedron* 73 (2017) 5624–5633 doi.org/10.1016/j.tet.2017.05.054.
- [42] a) Ş. Yaşar, T.K. Köprülü, Ş. Tekin, S. Yaşar, Synthesis, characterisation and cytotoxic properties of N-heterocyclic carbene silver(I) complexes, *Inorg. Chim. Acta* 479 (2018) 17–23 doi.org/10.1016/j.ica.2018.04.035; b) Ş. Yaşar, T.K. Köprülü, Ş. Tekin, S. Yaşar, Sulfonated N-heterocyclic carbene-silver (I) complexes: Synthesis, characterisation and biological evaluation, *Appl. Organomet. Chem.* 32 (2018) 4016, doi:10.1002/aoc.4016.
- [43] X. Liu, Z. Ma, J. Xing, H. Liu, Preparation and characterization of amino-silane modified superparamagnetic silica nanospheres, *J. Magn. Magn. Mater.* 270 (2004) 1–6, doi:10.1016/j.jmmm.2003.07.006.
- [44] Y. Huang, J. Tang, L. Gai, Y. Gong, H. Guang, R. He, H. Lyu, Different approaches for preparing a novel thiol-functionalized graphene oxide/Fe-Mn and its application for aqueous methylmercury removal, *Chem. Eng. J.* 319 (2017) 229–239, doi:10.1016/j.cej.2017.03.015.
- [45] X. Wang, H. Pan, Q. Lin, H. Wu, S. Jia, Y. Shi, One-step synthesis of nitrogen-doped hydrophilic mesoporous carbons from chitosan-based triconstituent system for drug release, *Nanoscale Res. Lett.* 14 (2019) 259, doi:10.1186/s11671-019-3075-y.
- [46] R. Aghaei, A. Eshaghi, Optical and superhydrophilic properties of nanoporous silica-silica nanocomposite thin film, *J. Alloys Compd.* 699 (2017) 112–118, doi:10.1016/j.jallcom.2016.12.327.
- [47] L.Q. Wu, Y.C. Li, S.Q. Li, Z.Z. Li, G.D. Tang, W.H. Qi, L.C. Xue, X.S. Ge, L.L. Ding, Study of cation distributions in spinel ferrites MxMn1-xFe2O4 (M=Zn, Mg, Al), *AIP Adv.* 5 (2015) 097210, doi:10.1063/1.4966253.
- [48] A.M.A. Imad, A.M. Barbara, Identification and paleoclimatic significance of magnetite nanoparticles in soils, *Proc. Natl Acad. Sci.* 18 (2018) 1736–1741, doi:10.1073/pnas.1719186115.
- [49] F. Heidari, M. Hekmati, H. Veisi, Magnetically separable and recyclable Fe₃O₄@SiO₂/isoniazide/Pd nanocatalyst for highly efficient synthesis of biaryls by Suzuki coupling reactions, *J. Colloid Interface Sci.* 501 (2017) 175–184, doi:10.1016/j.jcis.2017.04.054.
- [50] H. Günther, *NMR Spectroscopy: Basic Principles, Concepts and Applications in Chemistry*, third ed., Wiley-VCH, Weinheim, 2013.
- [51] D. Tapu, D.A. Dixon, C. Roe, 13C NMR spectroscopy of “Arduengo-type” carbenes and their derivatives, *Chem. Rev.* 109 (2009) 3385, doi:10.1021/cr800521g.
- [52] S. Yasar, M. Akkoc, N. Ozdemir, I. Ozdemir, Synthesis and catalytic activity of ionic palladium N-heterocyclic carbene complexes, *Turk J. Chem.* 43 (2019) 1622–1633, doi:10.3906/kim-1907-74.
- [53] M. Akkoc, F. Imik, S. Yasar, V. Dorcet, T. Roisnel, C. Bruneau, I. Ozdemir, An efficient protocol for palladium N-heterocyclic carbene-catalysed Suzuki-Miyaura reaction at room temperature, *Chem. Sel.* 2 (2017) 5729–5734, doi:10.1002/slct.201701354.
- [54] E.O. Karaca, M. Akkoc, S. Yasar, I. Ozdemir, Pd-N-heterocyclic carbene catalysed Suzuki-Miyaura coupling reactions in aqueous medium, *Arxiv* 5 (2018) 230, doi:10.24820/ark.5550190.p010.519.
- [55] Y. Dong, X. Wu, X. Chen, Y. Wei, N-Methylimidazole functionalized carboxymethylcellulose-supported Pd catalyst and its applications in Suzuki cross-coupling reaction, *Carbohydr. Polym.* 160 (2017) 106–114, doi:10.1016/j.carbpol.2016.12.044.
- [56] S. Sobhani, M.S. Ghasemzadeh, M. Honarmand, F. Zarifi, Acetamidine-palladium complex immobilized on γ-Fe₂O₃ nanoparticles: A novel magnetically separable catalyst for Heck and Suzuki coupling reactions, *RSC Adv.* 4 (2014) 44166–44174, doi:10.1039/C4RA04830J.
- [57] X. Wang, P. Hu, F. Xue, Y. Wei, Cellulose-supported N-heterocyclic carbene-palladium catalyst: Synthesis and its applications in the Suzuki cross-coupling reaction, *Carbohydr. Polym.* 114 (2014) 476–483, doi:10.1016/j.carbpol.2014.08.030.
- [58] H. Ke, X. Chen, G. Zou, N-Heterocyclic carbene/phosphite synergistically assisted Pd/C-catalyzed Suzuki coupling of aryl chlorides, *Appl. Organometal. Chem.* 28 (2014) 54–60, doi:10.1002/aoc.3076.
- [59] B. Karimi, P.F. Akhavan, A novel water-soluble NHC-Pd polymer: an efficient and recyclable catalyst for the Suzuki coupling of aryl chlorides in water at room temperature, *Chem. Commun.* 47 (2011) 7686–7688, doi:10.1039/C1CC00017A.
- [60] M. Khajehzadeh, M. Moghadam, A new poly(N-heterocyclic carbene Pd complex) immobilized on nano silica: an efficient and reusable catalyst for Suzuki-Miyaura, Sonogashira and Heck-Mizoroki C–C coupling reactions, *J. Organomet. Chem.* 863 (2018) 60–69, doi:10.1016/j.jorganchem.2018.03.030.